(Received 3 January 2024, Accepted 29 January 2024, Scheduled 23 February 2024)

A Single-Layer Filtering Slot Antenna Based on Circular SIW Cavity

Yinghang Chen[1], Xuehui Guan[1,*], Xianling Liang[2], Baoping Ren[1], and Shaopeng Wan[1]

[1]*School of Information Engineering, East China Jiaotong University, Nanchang 330013, China*
[2]*School of Electrical and Electronic Engineering, Shanghai Jiaotong University, Shanghai 200240, China*

ABSTRACT: A low profile and high selectivity filtering slot antenna based on circular substrate integrated waveguide (SIW) cavity is presented. The proposed antenna is originated from a circular SIW cavity operating at its TM_{010} mode. A cruciform slot is integrated on the top surface of the cavity, and the cavity is then split into four quarter-mode cavity resonators. In this aspect, the four similar quarter-TM_{010} modes will be generated by the compact structure. By amalgamating four similar modes into a single-band, the bandwidth of antenna is widened. Based on the structure, a filtering slot antenna with central frequency of 8 GHz and bandwidth of 5.6% is designed and fabricated. Measured results agree well with the simulated ones. In addition, two radiation nulls are produced at the edges of the passband, and the selectivity in the transition band is enhanced greatly.

1. INTRODUCTION

With the promotion of modern radar and communication applications, multifunctional devices are in tremendous requirement. Within the RF front end, antennas and filters are two irreplaceable elements. Nevertheless, the separate installation of filters and antennas results in a larger overall size and increased insertion loss [1–3]. When it comes to wireless systems, the strategic integration of antennas and filters results in a more compact RF front end and an enhancement in the system's overall performance [4].

In contrast to microstrip filtering antennas, substrate integrated waveguide (SIW) filtering antennas are currently under extensive investigation due to their superior qualities, including higher quality factor, increased power-handling capacity, and reduced losses. In [5], a square patch monopole antenna is cascaded to a SIW filter to form a filtering antenna. Due to the additional filtering circuits, relatively complex structures are inevitable, and the difficulty of processing and assembly also increases. In this respect, when the filter and antenna are unified into a single module, it leads to a decrease in the size and weight of the RF front-end. Through the replacement of the load with a radiator, a filter can be transformed into a filtering antenna. The SIW technique facilitates integration with planar circuits [6]. In [7], an antenna with fourth-order wideband filtering capabilities, constructed from two dual-mode SIW cavities, is presented. The zeros of the transmission coefficient S_{21} are found as radiation nulls (RNs) in the gain.

The SIW can be split along an imaginary quasi-magnetic boundary, transforming into a half-mode SIW (HMSIW). The HMSIW maintains a field distribution that closely resembles that of the original SIW. In [8], a long slot on the SIW cavity divides the TE_{110}-mode cavity into two half-mode ones, where mixed electric and magnetic coupling is introduced between HMSIW resonator and the upper patch, thus good radiation performance with radiation nulls is achieved. In [9], a low-profile single-layer duplex-filtering antenna is proposed. Acting as an HMSIW resonator, the SIW cavity emits radiation through an additional longitudinal slot and the open-end of the HMSIW. In order to achieve a size reduction in the SIW filtering antenna, the HMSIW can be once more split into two sections along its symmetry plane, forming what is known as a quarter-mode SIW (QMSIW). Hence, in [10], utilizing two slots on the square SIW cavity, three radiating modes are employed, consisting of one half-mode (HM) and two quarter-modes (QMs), to realize an antenna with an enhanced bandwidth for its operational band. However, only one radiation null in the upper sideband is realized, and the lower sideband shall be improved. In the previously mentioned designs, the filtering response without sufficient RNs is the main problem of SIW-based filtering slot antennas. Therefore, it is still a challenging task to design SIW filtering slot antennas with high selectivity using QMSIW cavity.

In this letter, a compact circle single-layer SIW hybrid filtering antenna is proposed. The top surface of the circular SIW cavity features a cruciform slot, and the structure is split into four quarter-mode cavity resonators. Four resonant modes are applied to raise the impedance width and elevate the selectivity of the antenna. Radiation nulls are formed in the two sidebands of the antenna, which contribute to an increased level of selectivity for the antenna. The filtering slot antenna is fabricated and measured.

2. CONSTRUCTION OF ANTENNA

Figure 1 presents the geometry of proposed filtering antenna. The proposed antenna is formed by a circular SIW cavity and a pair of orthogonal slots. The horizontal slot with width of W_1

* Corresponding author: Xuehui Guan (xuehuiguan@gmail.com).

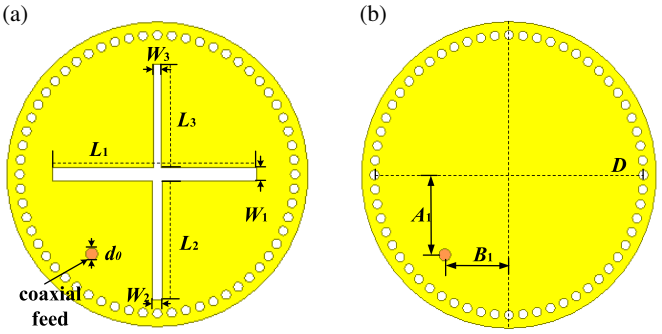

FIGURE 1. Geometry of the proposed filtering antenna. (a) Top view. (b) Bottom view. $D = 23.0$, $L_1 = 15.6$, $W_1 = 1$, $L_2 = 9.5$, $W_2 = 1$, $L_3 = 7.8$, $W_3 = 0.6$, $A_1 = 6$, $B_1 = 5.5$, $d_0 = 0.8$, and $p = 0.7$ (unit: mm).

and length of L_1 of the antenna is the main radiator. Two vertical slots with widths of W_2 and W_3 are loaded to the center of the horizontal slot. A coaxial feed is attached to one quarter-mode cavity. In the design, a substrate of Rogers 5880 is utilized, which has a relative dielectric constant of 2.2 and a thickness of 0.508 mm.

The frequency of resonating mode in the SIW cavities is determined by [12]

$$f_{nm0} = \frac{c}{2\pi\sqrt{\mu_r\varepsilon_r}} \cdot \frac{P_{nm}}{R_{eff}} \tag{1}$$

where c is the speed of light in a vacuum, and ε_r and μ_r are the relative permittivity and relative permeability of substrate, respectively. P_{nm} is the mth-root of the Bessel function of the first kind with order n [13]. R_{eff} denotes the effective radius of the circular cavity, that is

$$2R_{eff} = 2R - \frac{d^2}{0.95p} \tag{2}$$

where R is used to signify the radius, and R_{eff} represents the effective radius of the standard circular cavity. Furthermore, d denotes the diameter of vias, while p signifies the gap among the vias. To minimize electromagnetic energy leakage and ensure stability of structural, it is necessary for p and to d adhere to the conditions of $p < 2d$.

Typical values of P_{nm} and their corresponding resonant frequencies of high-order modes are calculated and provided in Table 1. As shown in Table 1, for TM_{010} mode, P_{nm} is 2.405, and its resonant frequency is 8.7 GHz. Due to the influence of slot, the center frequency will shift towards lower frequencies, resulting in a partial deviation between the theoretical value and actual center frequency.

TABLE 1. Typical values of P_{nm}.

n/m	1	2	3
0	2.405	5.520	8.654
1	3.832	7.016	10.174
2	5.135	8.417	11.620
3	6.380	9.761	13.015

3. FOURTH-ORDER FILTERING ANTENNA

To effectively elucidate the proposed antenna and its design concept, two types of transitional SIW filtering slot antennas are explored. The structures of three antennas are shown in Fig. 2, comprising Ant. I and Ant. II, i.e., a third-order SIW antenna with slots 1 and 2 for better selectivity. For comparison, the proposed filtering slot antenna is also provided in Fig. 2(c).

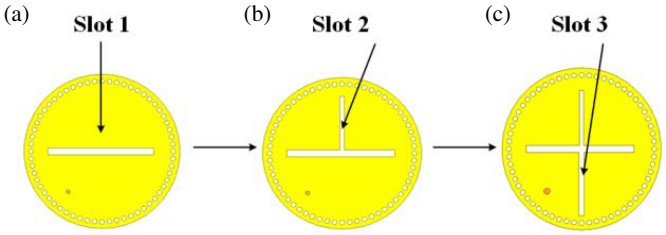

FIGURE 2. Top surface of the evolution process. (a) Ant. I. (b) Ant. II. (c) Proposed antenna.

The improved filtering antenna is sourced from a SIW slot Ant. I. As shown in Fig. 2(a), a horizontal slot is placed in the center of the cavity, and two half-mode resonances and a radiation null are produced. To produce an additional resonance, slot 2 is placed on the higher half cavity, as shown in Fig. 2(b), and one half-mode resonance is split into two quarter-mode resonances. By the same token, slot 3 is etched on the lower half cavity, and the other half-mode resonance is also split into two quarter-mode resonances. the fourth order SIW filtering antenna is obtained.

Slot 1, slot 2, and slot 3 are all etched concurrently on the top of the SIW cavity, as depicted in Fig. 2(c), in order to achieve an antenna with a high level of selectivity. The fourth-order filtering antenna is completed, featuring radiation nulls on either side of passband, as depicted by the solid line in Fig. 3.

4. COUPLING TOPOLOGY

To disclose the modes associated with the four resonances, an investigation of the distributions of electric field is executed. In Fig. 4, the fields of the four resonances are separately located in various quarter-circle sides of the cavity. The electric field intensity diminishes from the center to the outermost edge. As shown in Fig. 4(b) and Fig. 4(c), slot 1 is the main radiator, which generates quarter-TM_{010} modes. As depicted in Fig. 4(a) and Fig. 4(d), the electric fields are predominantly situated in the vicinity of the cruciform slot and core of the cavity.

The coupling topology of the proposed antenna is provided in Fig. 5, where resonators 1, 2, 3, and 4 indicate the four quarter-mode SIW cavities. The slot functions as the load (L) to the resonators, and S indicates the feeding. Each mode couples to the slot, and the coupling topology becomes something complicated. Two radiation nulls are created at the lower and upper edges of the working band, and the selectivity of the antenna is improved.

Due to the complexity of the coupling between each quarter mode cavity and radiation slot, it is very difficult to extract their exact coupling values, thus parameter sweep is conducted on

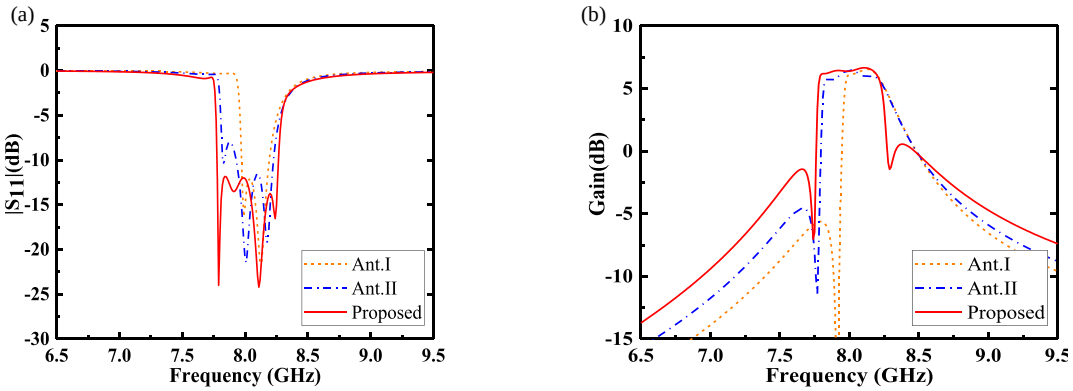

FIGURE 3. Frequency response simulations of the three mentioned antennas, encompassing (a) S_{11} and (b) gain in the zenith direction.

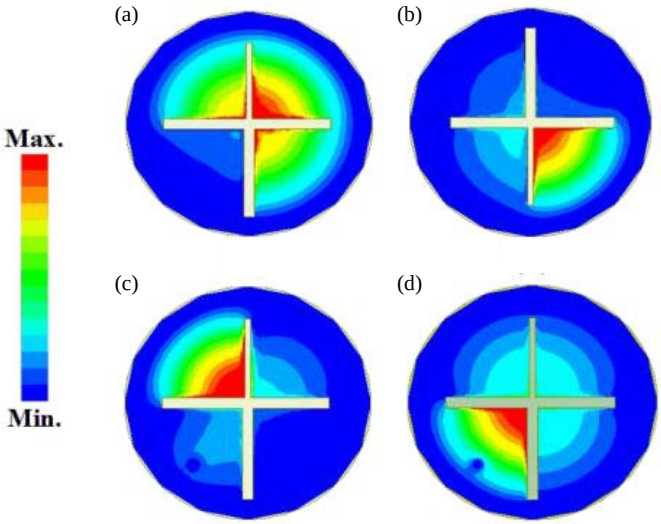

FIGURE 4. Simulated electric-field distributions of the proposed antenna at (a) 7.79 GHz, (b) 7.92 GHz, (c) 8.11 GHz, and (d) 8.24 GHz.

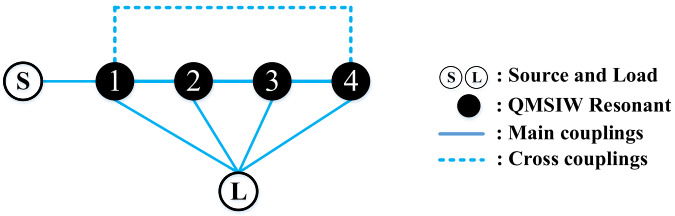

FIGURE 5. Coupling topology of the proposed antenna.

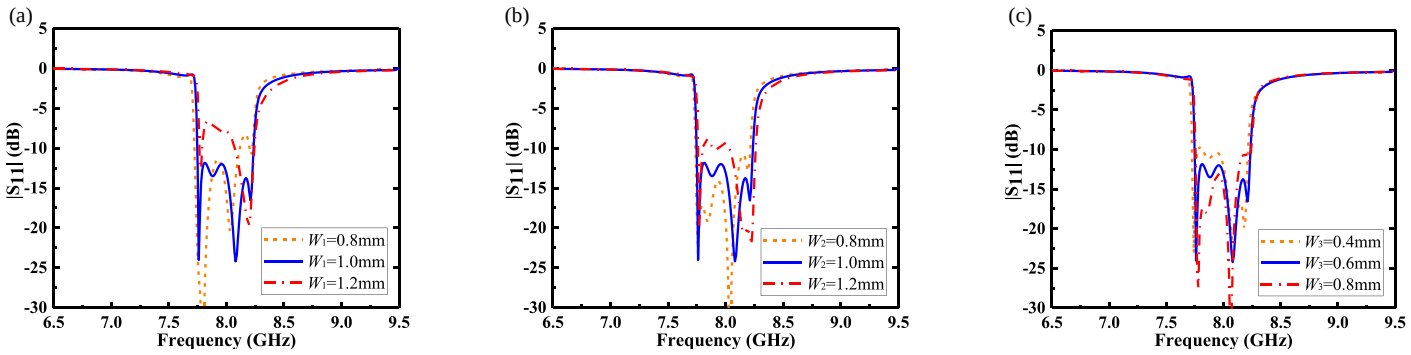

FIGURE 6. Variation of reflection coefficients versus (a) W_1, (b) W_2, and (c) W_3.

the width of the slots. The variations of reflection coefficients versus W_1, W_2, and W_3 are provided in Fig. 6. The next key issue that needs to be addressed is the selection of location of coaxial feed in the antenna. Actually, the position of the feeding point in the SIW cavity is determined by the desired external coupling or the input impedance at the feeding point. When the feeding point is located at the center of the quarter-mode SIW cavity, the input impedance reaches its maximum value. The final position of feeding point is optimized by tuning A_1 and B_1.

5. EXPERIMENTAL RESULTS AND DISCUSSIONS

A SIW filtering slot antenna characterized by its straightforward and space-efficient construction is proposed. Based on a circle SIW filtering structure, a fourth-order filtering slot

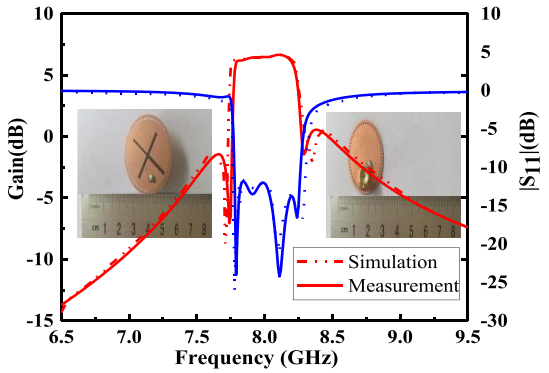

FIGURE 7. Simulated and measured S_{11} and gain of the antenna.

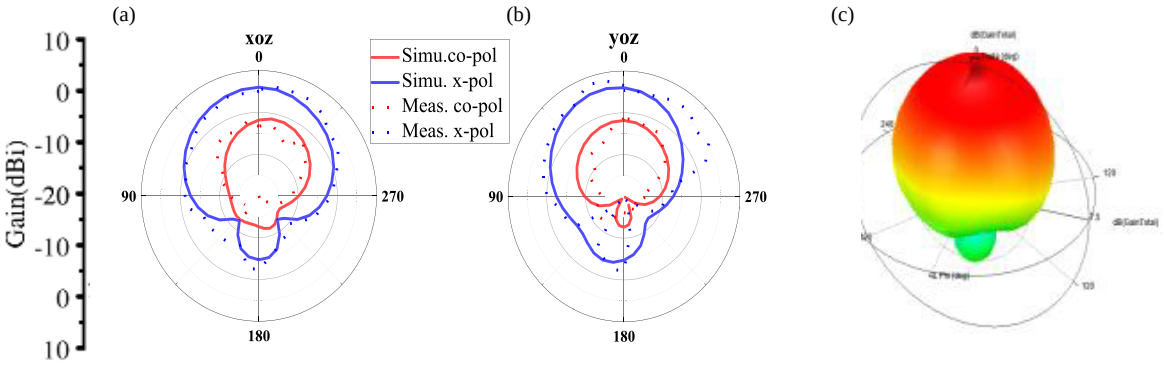

FIGURE 8. Simulated and measured normalized radiation patterns of the proposed filtering antenna at 7.92 GHz. (a) xoz plane. (b) yoz plane. (c) 3D radiation diagram.

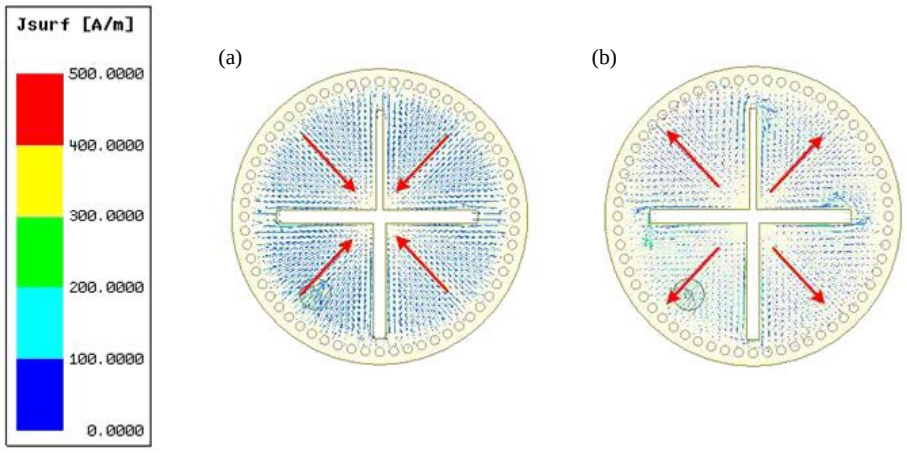

FIGURE 9. Simulated current distributions of the proposed antenna with frequency at (a) the lower radiation null, and (b) the upper radiation null.

antenna with central frequency of 8 GHz and bandwidth of 5.6% is designed and fabricated. The final obtained parameters of the proposed filtering slot antenna are: $L_1 = 15.6$ mm, $L_2 = 9.5$ mm, $L_3 = 7.8$ mm, $W_1 = 1$ mm, $W_2 = 1$ mm, and $W_3 = 0.6$ mm. An Agilent N5230A vector network analyzer is employed to measure its reflection coefficient, while the near-field antenna test system is used to obtain radiation patterns and gains.

The simulated and measured S_{11} values as well as gains across the frequency range are shown in Fig. 6. Based on the measurements, there is a -10 dB that covers 5.6% of the frequency range, from 7.79 to 8.24 GHz, slightly wider than the simulated bandwidth. Additionally, there is a consistent realized gain ranging from 6.15 to 6.65 dB in the broadside direction across the operating frequency range. Besides, the radiation nulls at 7.74 GHz and 8.30 GHz are clearly found at the two edges of the working frequency range. Fig. 7 (measurement picture) shows superior selectivity and a steep drop-off in the frequency response. The photo of the manufactured antenna is presented in the inset of Fig. 7. The normalized radia-

TABLE 2. Comparison of previous single-layer filtering antennas.

Ref.	f_0 (GHz)	FBW (%)	Gain (dB)	Num. of Orders/Cavities	Num. of TZs	Circuit Size ($\lambda_g \times \lambda_g$)
[11]	3.5	9.14	6.4	3/1	2	0.74×0.74
[14]	9.5	2.53	5.8	2/1	2	0.61×0.8
[15]	3.5	5.1	7.0	4/1	2	0.53×0.81
[16]	2.75	5.1	6.3	2/2	2	0.33×0.33
[17]	3.71	8.29	5.1	3/1	1	0.55×0.87
[18]	11.8	11.84	5.0	3/1	2	0.48×0.47
[20]	6.65	3.2	9.2	3/1	1	1.33×1.33
[21]	8.3	6.02	6.63	2/1	4	1.17×0.70
This work	8.0	5.6	**6.65**	**4/1**	2	**0.307×0.307**

tion patterns of the proposed filtering antenna about simulated and measured are given in Fig. 8. On the whole, the simulated and measured results are in close alignment across the complete operating frequency spectrum. In comparison with alternative designs, the antenna utilizes only a single substrate layer, resulting in an expanded operational bandwidth.

Figure 9(a) shows that the current is predominantly concentrated across the boundary of the SIW. Top surface currents of the cruciform slot are opposite to each other. The offsetting current distributions will annul the effects on the broadwall radiating slot, establishing a lower null. In Fig. 9(b), when considering the direction, it can be inferred that the radiation can counteract that in the broadside, resulting in the creation of the upper null.

Table 2 presents a performance assessment of the filtering antenna in comparison to other filtering antennas. The proposed antenna combines the largest quantity of modes within a compact structure.

Figure 10 shows the measured total radiation efficiency of the proposed antenna. The fabricated antenna achieves a high efficiency of around 87% across the working band.

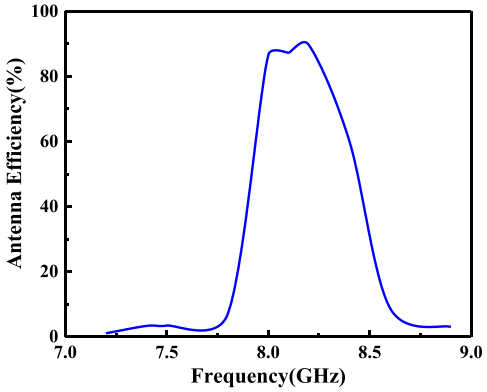

FIGURE 10. Measured antenna efficiency.

Antenna efficiency is determined by

$$\eta = \frac{\text{Gain}}{D_{\max}} \tag{3}$$

According to [19], the gain and $D_{\max}$ represent the measured gain and the maximum available directivity.

6. CONCLUSION

In this letter, a concise description is provided for a single-layer filtering antenna, while cruciform slots feature on the top surface. The designed antenna is implemented by a SIW cavity and one cruciform slot. The purpose of slot 1 is to introduce a radiation null, improving the filtering response, while both slot 2 and slot 3 are responsible for introducing an additional resonance within the operating band to expand the bandwidth and create an additional radiation null. The measured results correspond to the simulations. In contrast to various other filtering antennas, the suggested design, featuring just one resonant cavity, meets the requirements for RF system integration, miniaturization, and multifunction.

ACKNOWLEDGEMENT

This work is supported by the National Natural Science Foundation of China (No. 62361025, No. 62261022), in part by the Science and Technology Plan Project of Jiangxi Province (No. 20204BCJ23007, No. 20202ACBL212002), and in part by the Project of State Key Laboratory of Millimeter Wave (No. K202114).

REFERENCES

[1] Zhang, X. Y., W. Duan, and Y.-M. Pan, "High-gain filtering patch antenna without extra circuit," *IEEE Transactions on Antennas and Propagation*, Vol. 63, No. 12, 5883–5888, Dec. 2015.

[2] Duan, W., X. Y. Zhang, Y.-M. Pan, J.-X. Xu, and Q. Xue, "Dual-polarized filtering antenna with high selectivity and low cross polarization," *IEEE Transactions on Antennas and Propagation*, Vol. 64, No. 10, 4188–4196, Oct. 2016.

[3] Jin, J. Y., S. Liao, and Q. Xue, "Design of filtering-radiating patch antennas with tunable radiation nulls for high selectivity," *IEEE Transactions on Antennas and Propagation*, Vol. 66, No. 4, 2125–2130, Apr. 2018.

[4] Luo, G. Q., W. Hong, H. J. Tang, J. X. Chen, X. X. Yin, Z. Q. Kuai, and K. Wu, "Filtenna consisting of horn antenna and substrate integrated waveguide cavity FSS," *IEEE Transactions on*

Antennas and Propagation, Vol. 55, No. 1, 92–98, Jan. 2007.

[5] Adhikary, M., A. Sarkar, A. Sharma, A. Biswas, and M. J. Akhtar, "Miniaturized SIW filter antenna with loadable sensor for various microwave sensing applications," in *2017 IEEE International Symposium on Antennas and Propagation & USNC/URSI National Radio Science Meeting*, 2505–2506, San Diego, CA, USA, Jul. 2017.

[6] Nova, O. A., J. C. Bohorquez, N. M. Pena, G. E. Bridges, L. Shafai, and C. Shafai, "Filter-antenna module using substrate integrated waveguide cavities," *IEEE Antennas and Wireless Propagation Letters*, Vol. 10, No. 1, 59–62, Jan. 2011.

[7] Xie, H.-Y., B. Wu, Y.-L. Wang, C. Fan, J.-Z. Chen, and T. Su, "Wideband SIW filtering antenna with controllable radiation nulls using dual-mode cavities," *IEEE Antennas and Wireless Propagation Letters*, Vol. 20, No. 9, 1799–1803, Sep. 2021.

[8] Fan, C., B. Wu, Y.-L. Wang, H.-Y. Xie, and T. Su, "High-gain SIW filtering antenna with low H-plane cross polarization and controllable radiation nulls," *IEEE Transactions on Antennas and Propagation*, Vol. 69, No. 4, 2336–2340, Apr. 2021.

[9] Kumar, A. and A. A. Althuwayb, "SIW resonator-based duplex filtenna," *IEEE Antennas and Wireless Propagation Letters*, Vol. 20, No. 12, 2544–2548, Dec. 2021.

[10] Niu, B.-J. and J.-H. Tan, "Low-profile SIW cavity antenna with enhanced bandwidth and controllable radiation null," *Microwave and Optical Technology Letters*, Vol. 62, No. 5, 2014–2018, May 2020.

[11] Liu, Q., L. Zhu, J. Wang, and W. Wu, "A wideband patch and SIW cavity hybrid antenna with filtering response," *IEEE Antennas and Wireless Propagation Letters*, Vol. 19, No. 5, 836–840, May 2020.

[12] Peng, Y., Y. Mai, W. Xu, J. Wang, B. Yu, and H. Zhang, "Dual-band semi-circular HMSIW cavity antenna using higher-order modes," in *2019 International Symposium on Antennas and Propagation (ISAP)*, 1–3, Xi'an, China, Oct. 2019.

[13] Pozar, D. M., *Microwave Engineering*, 2nd ed., Wiley, 1998.

[14] Wang, C., X. Wang, H. Liu, Z. Chen, and Z. Han, "Substrate integrated waveguide filtenna with two controllable radiation nulls," *IEEE Access*, Vol. 8, 120 019–120 024, Jun. 2020.

[15] Li, D. and C. Deng, "A single-layer filtering antenna with two controllable radiation nulls based on the multimodes of patch and SIW resonators," *IEEE Antennas and Wireless Propagation Letters*, Vol. 22, No. 3, 551–555, Mar. 2023.

[16] Hu, K.-Z., M.-C. Tang, D. Li, Y. Wang, and M. Li, "Design of compact, single-layered substrate integrated waveguide filtenna with parasitic patch," *IEEE Transactions on Antennas and Propagation*, Vol. 68, No. 2, 1134–1139, Feb. 2020.

[17] Lovato, R. and X. Gong, "A third-order SIW-integrated filter/antenna using two resonant cavities," *IEEE Antennas and Wireless Propagation Letters*, Vol. 17, No. 3, 505–508, Mar. 2018.

[18] Yin, J.-Y., T.-L. Bai, J.-Y. Deng, J. Ren, D. Sun, Y. Zhang, and L.-X. Guo, "Wideband single-layer substrate integrated waveguide filtering antenna with U-shaped slots," *IEEE Antennas and Wireless Propagation Letters*, Vol. 20, No. 9, 1726–1730, Sep. 2021.

[19] Zhang, T., L. Chen, A. U. Zaman, and J. Yang, "Ultra-wideband millimeter-wave planar array antenna with an upside-down structure of printed ridge gap waveguide for stable performance and high antenna efficiency," *IEEE Antennas and Wireless Propagation Letters*, Vol. 20, No. 9, 1721–1725, Sep. 2021.

[20] Jung, E.-Y., J. W. Lee, T. K. Lee, and W.-K. Lee, "SIW-based array antennas with sequential feeding for X-band satellite communication," *IEEE Transactions on Antennas and Propagation*, Vol. 60, No. 8, 3632–3639, Aug. 2012.

[21] Hao, Z. C., X. Liu, X. Huo, and K. K. Fan, "Planar high-gain circularly polarized element antenna for array applications," *IEEE Transactions on Antennas and Propagation*, Vol. 63, No. 5, 1937–1948, May 2015.